Inhibition of HIV-1 Envelope-Mediated Fusion by Synthetic Batzelladine Analogues†

Carole A. Bewley,*,‡ Satyajit Ray,‡ Frederick Cohen,§ Shawn K. Collins,§ and Larry E. Overman*,§

Laboratory of Bioorganic Chemistry, National Institute of Diabetes and Digestive and Kidney Diseases, National Institutes of Health, DHHS, Bethesda, Maryland 20892, and Department of Chemistry, 516 Rowland Hall, University of California, Irvine, California 92697-2025

Received January 22, 2004

Marine natural products that feature polycyclic guanidine motifs, such as crambescidins and batzelladines, are known to have antiviral activities toward some viruses including HSV and HIV. In this study we evaluated a synthetic library containing 28 batzelladine analogues, the structures of which encompass and surpass variations seen in natural batzelladines, for their ability to inhibit HIV-1 envelope-mediated cell−cell fusion. Clear structure−activity relationships were revealed and indicated that the best inhibitors of fusion were most similar in structure to natural batzelladine F, with IC_{50} values ranging from 0.8 to 3.0 μM. Proceeding from the earlier finding that some batzelladines block gp120-CD4 binding, modeling studies of inhibitors binding to the CD4 binding site on gp120 were carried out. The lowest energy models suggest a preferred orientation for inhibitor binding that is consistent with the observed structure−activity relationships.

A number of marine invertebrates, especially sponges belonging to the genera *Batzella* and *Crambe*, are known to produce complex secondary metabolites that contain one or more polycyclic guanidine units. Instructive examples include members of the crambescidin family (such as **1** and **2**) that feature a pentacyclic guanidine core coupled to alkyl spermidine moieties,[1−5] and the batzelladine family[6,7] (examples include **5**−**10**), members of which generically comprise mixed bicyclic and/or tricyclic guanidine units, with the bisguanidines tethered by an alkyl ester unit (Figure 1). Fervent interest in this group of compounds arises from the combination of notable biological activities associated with these compounds, as well as the synthetic challenges posed by these complex structures.

The biological activities associated with the crambescidins are varied, and reports have included cytotoxicity toward the cancer cell lines P388,[1] L1210,[2,3] and HCT-16,[4] antifungal activity toward *Candida albicans*,[1] and antiviral activities toward Herpes simplex virus type 1 (HSV-1)[2,3] and human immunodeficiency viruses (HIV).[6,8] Batzelladines A−E, on the other hand, were originally discovered in an enzyme-linked immunosorbent assay (ELISA) for their ability to block interactions between the surface envelope glycoprotein of HIV, namely gp120, and the extracellular domains of its primary receptor CD4.[6] Later, the structures of batzelladines F−I were determined following the observation that crude extracts of the *Batzella* sp. were able to induce dissociation of the complex between the protein tyrosine kinase $p56^{lck}$ and CD4.[7] It is worth emphasizing that although both of these assays in which the batzelladines proved active involve CD4, the regions on CD4 with which gp120 and $p56^{lck}$ interact are distinct, with gp120 binding to the extracellular regions of CD4 and $p56^{lck}$ binding to the intracellular cytoplasmic tail of CD4.

As part of an effort to discover natural products that can block protein−protein interactions comprising large surfaces, such as those involved in HIV-1 entry into its host cell, we recently described new analogues of the crambescidin family, crambescidin 826 (**2**) and dehydrocrambine A (**3**).[5] Demonstrations that these alkaloids inhibit HIV-1 envelope-mediated cell fusion (or HIV entry) in a time-dependent manner and exert their effect through interactions with HIV-1 envelope (Env) rather than cellular receptors suggested that, like the structurally related batzelladines, crambescidins may be able to block CD4-gp120 interactions. To further evaluate the specific structural requirements for guanidine alkaloids as HIV-1 fusion inhibitors, we describe here the results of testing a series of 28 synthetic batzelladine analogues (**11**−**38**) in an HIV-1 cell fusion assay. Clear structure−activity relationships were revealed suggesting a model for polycyclic guanidine alkaloids binding to the HIV-1 surface envelope glycoprotein gp120. These results together with modeling studies are presented.

Results and Discussion

Structure−Activity Relationships of Batzelladine Analogues as Fusion Inhibitors. Common to all of the batzelladines is the presence of a tricyclic guanidine unit. Internally, these ring systems vary in the number and positioning of double bonds within the pyrimidine rings, as well as in the stereochemistry of the angular hydrogens flanking the pyrrolidine nitrogen (Figure 1). In addition to variations within the tricyclic unit itself, the natural products differ in location and configuration of varied alkyl substituents. Following the discovery of batzelladines and crambescidins, several synthetic approaches to building these polycyclic guanidine ring systems have been described.[9−13] As a result of work from the Overman group, a library of batzelladine analogues that encompasses and surpasses variations seen in the natural products[14,15] has been synthesized and is illustrated in Figure 2. The assemblage of structures comprising this library allowed us to evaluate the contribution toward inhibitory activity by several different structural features. These include the type (bicyclic or tricyclic) and number of guanidine ring systems (one or two) present, the absolute configuration of these units, and the position and number of alkyl

† Dedicated to the late Dr. D. John Faulkner (Scripps) and the late Dr. Paul J. Scheuer (Hawaii) for their pioneering work on bioactive marine natural products.

* To whom correspondence should be addressed. (C.A.B.) Tel: 301-594-5187. Fax: 301-402-0008. E-mail: caroleb@mail.nih.gov. (L.E.O.) Tel: 949-824-6793. Fax: 949-824-3866. E-mail: leoverma@uci.edu.

‡ National Institute of Diabetes and Digestive and Kidney Diseases.

§ University of California.

10.1021/np049958o CCC: $27.50
Published on Web 07/08/2004

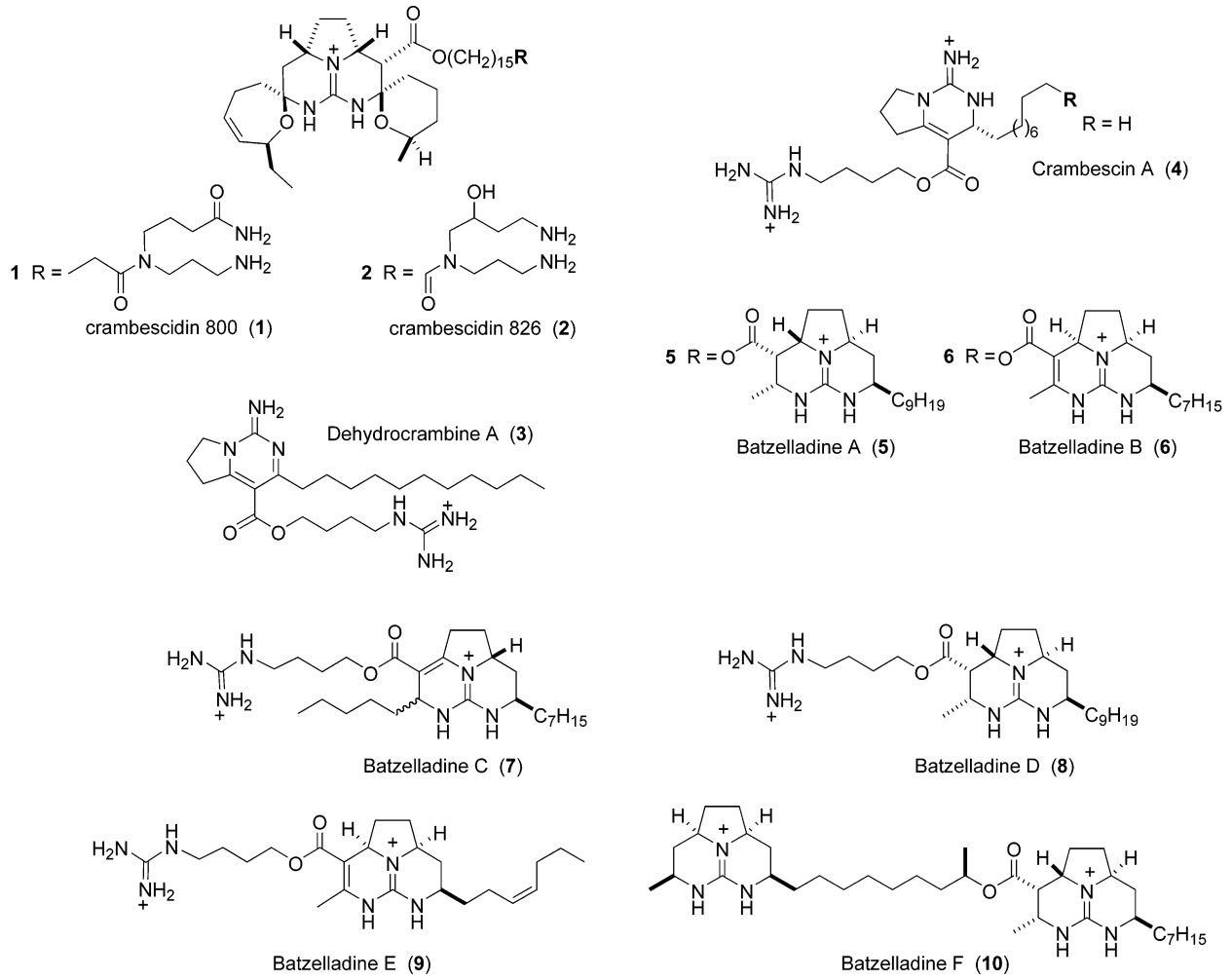

Figure 1. Examples of crambescidins and batzelladines.

substituents decorating the guanidine core. For those compounds containing two guanidine units, the rigidity of the linker tethering the two ring systems also could be evaluated.

Each of these compounds was tested in an HIV-1 Env-mediated cell−cell fusion assay for their ability to inhibit fusion.[16] Compounds were tested against both X4 and R5 HIV-1 strains and included LAV and SF162, respectively. Initially, compounds were tested at single concentrations of 100 and 5 μM toward both viral strains. Data generated from the assays carried out in the presence of 100 μM concentrations yielded little to no structural information because most of the compounds tested inhibited fusion greater than 80% (data not shown). However, in the presence of 5 μM inhibitor, clear structure−activity relationships were evident, as the percent fusion observed ranged from 0 to 100% at these concentrations (Figure 3). After these initial assays, dose−response curves were measured for selected compounds to better deduce structure−activity relationships (Table 1). Representative inhibition curves for compounds **13**, **22**, **25**, and **27** are shown in Figure 4.

Analogues viewed as monomers in terms of the number of guanidine motifs appear in the left panel of Figure 2. Compounds **11** and **12** contain a bicyclic ring system and terminal benzyloxy group, and compounds **13**−**21** feature a single tricyclic guanidine motif. Of these tricyclics, the β-keto esters **13**, **14**, and **16** bear a C-1′ alkyl side chain, and compound **15** contains a C-2′ ester substituent in addition to a C-1′ alkyl side chain. Compounds **17**−**19** comprise a core similar to that of batzelladine D (**8**) and unlike **13**−**16** are substituted by carboxyl groups in addition to the C-1′ alkyl chain. Analogues **22**−**24** contain one bicyclic and one tricyclic guanidine unit, with the bicyclic ring system connected by an alkyl ester group off C-1′ of the tricyclic motif, and compounds **25**−**30**, which closely resemble natural batzelladine F,[15] are alike in that they contain two tricyclic guanidine motifs where both ring systems bear an alkyl group at C-1′. Seen in the right-most column of Figure 2, the bistricyclic compounds **31**−**38** are distinguished by the presence of a C_7 or C_9 alkyl chain at C-1 rather than the C-1 methyl group present in all other tricyclic guanidine analogues. Further variations among compounds **31**−**38** not seen in the natural products include the presence of biscarboxy esters in **31**−**33** and **36**−**38** and a 1,4-benzenedimethanol linker connecting the two tricyclic units in **37** and **38**.

The fusion data in Figure 3 indicate that these compounds generally fall within three activity levels, those inhibiting greater than 90%, those inhibiting greater than approximately 40%, and those inhibiting less than approximately 20%, at 5 μM concentrations. In terms of structure−activity relationships, all compounds with C-1 alkyl substituents larger than methyl (**20**, **31**−**38**) were inactive, indicating that only a small substituent at this position is tolerated. Notably, in the fusion assays employing 100 μM inhibitor, compounds **37** and **38** were also inactive, indicating that the added rigidity is detrimental to binding to gp120. Structures of compounds that were modest inhibitors of fusion were varied and included mono-

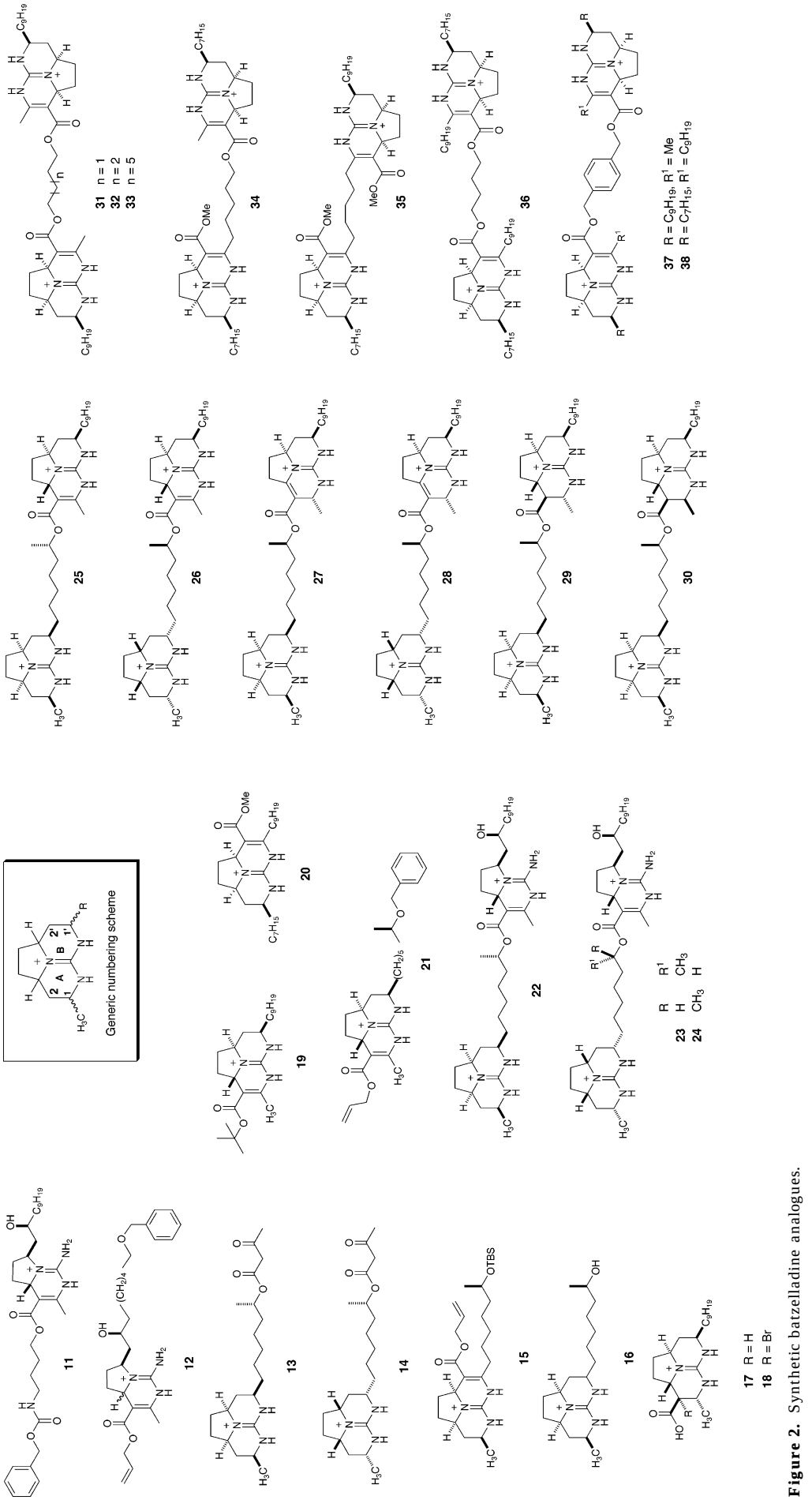

Figure 2. Synthetic batzelladine analogues.

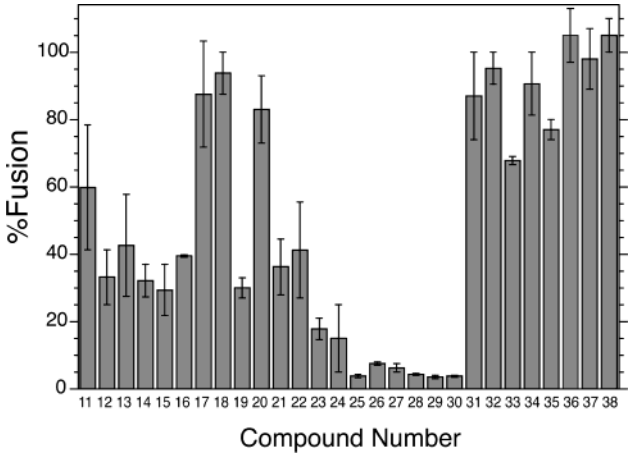

Figure 3. Inhibition of HIV-1 envelope-mediated fusion for analogues **11**−**38** tested at 5 μM concentration.

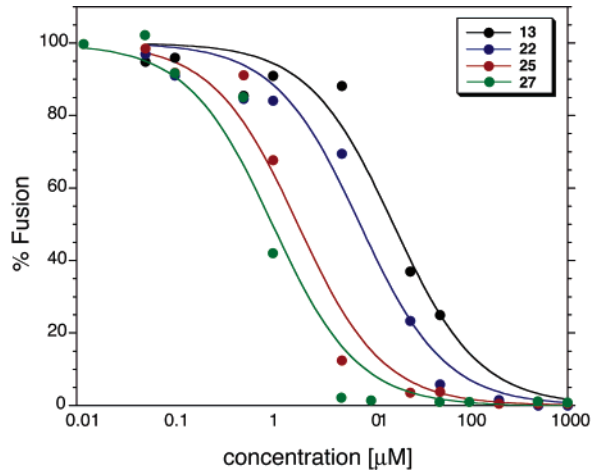

Figure 4. Representative inhibition curves for HIV-1 Env-mediated fusion. Curves for compounds **13**, **22**, **25**, and **27** are represented by solid black, blue, red, and green circles, respectively.

Table 1. IC_{50} Values for Selected Analogues[a]

compound	IC_{50} values[b]
13	17.0 ± 3.3
14	5.3 ± 0.7
15	4.5 ± 0.9
19	3.5 ± 0.6
22	7.7 ± 1.5
24	6.2 ± 1.2
25	1.8 ± 0.4
27	0.8 ± 0.2
29	3.0 ± 0.6
30	2.5 ± 0.6

[a] Dose−response curves were determined on analogues for which sufficient quantities of compound were available. [b] Micromolar.

and bisguanidines **12**−**16**, **19**, and **21**−**24**. By far the most active compounds among this library are compounds **25**−**30**, all of which contain two tricyclic guanidine motifs connected by an alkyl ester linkage comprising eight heavy atoms. Although compounds **25**−**30** can be viewed as having the same carbon skeletons, the absolute and relative configuration of the left-hand guanidine ring system differs. When considered together, these results suggest that for this class of compounds the structures of the best fusion inhibitors are pseudo-dimers incorporating two tricyclic guanidine motifs connected by a flexible linker with each of the guanidine units bearing a methyl group at C-1 and an alkyl group at C-1′. These structures are most similar to the natural products batzelladines F and G.[7,15]

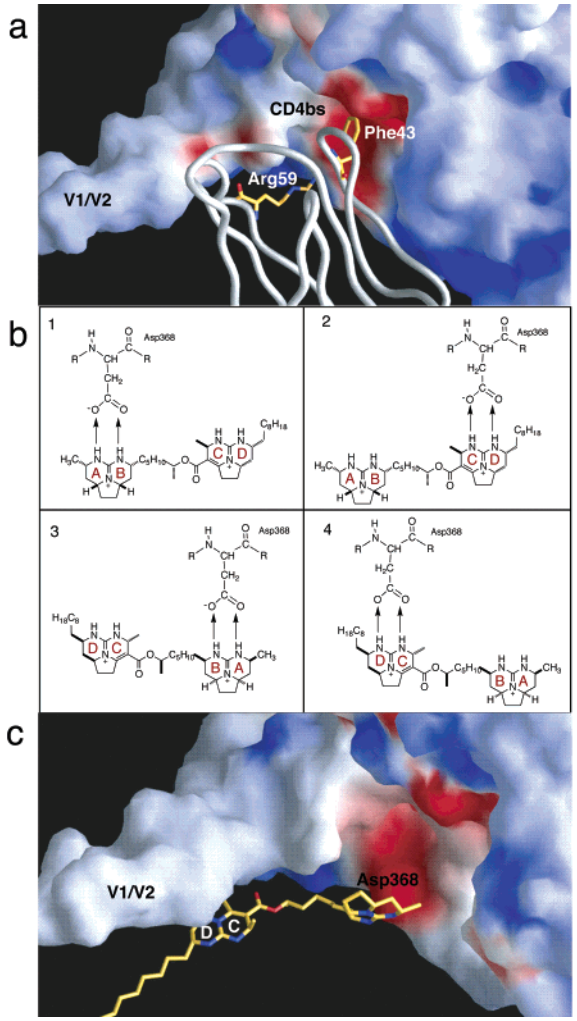

Figure 5. Complexes and binding orientations for gp120. (a) CD4-gp120 complex with gp120 shown in a charged surface representation with negative and positive regions colored red and blue, respectively; CD4 shown in a Cα worm representation, with Phe 43 and Arg 59 shown as rods with nitrogen and oxygen atoms colored blue and red, respectively. (b) Four possible orientations in which bisguanidine analogues can bind to gp120. Note that manual docking indicates this type of inhibitor can best be accommodated in the CD4 binding site in a nearly horizontal position, as viewed in this figure. Positions closer to vertical are precluded by the amino acid residues appearing at the top of the binding site, in the views shown here. (c) Model of the preferred orientation (box 3 of 5b) of compound **27** binding to gp120. The guanidine group of rings A and B are within hydrogen-bonding distances of the carboxylate of Asp 368.

Modeling of Batzelladine Analogues Binding to gp120. The initial steps leading to HIV-1 virus−cell or cell−cell fusion include attachment of the viral surface envelope glycoprotein gp120 to the cellular receptor CD4, which further permits binding of gp120 to one of two classes of co-receptors. This assembly ultimately facilitates fusion between the virus and cell membranes.[17] The first series of batzelladines, A−E, were discovered in an ELISA format that detects binding of the HIV-1 surface envelope (Env) glycoprotein gp120 binding to the primary receptor CD4.[6] Batzelladines A and B inhibited gp120-CD4 binding at low micromolar concentrations, as well as inhibiting HIV infectivity, as would be expected for a fusion inhibitor. The crystal structure of a ternary complex comprising CD4, a deglycosylated core construct of gp120, and a neutralizing antibody known as 17b revealed unique features of the CD4-gp120 interface (Figure 5a).[18] In terms of gp120, the CD4 binding site (CD4bs) comprises a substantial binding pocket that is formed by both hydrophobic and polar amino

acid residues including a key aspartic acid, Asp 368. On the CD4 side, although numerous amino acids are involved in binding to gp120, two amino acids, namely, Phe 43 and Arg 59, dominate the intermolecular contacts. Phe 43 is involved in van der Waals contacts with hydrophobic regions of the CD4bs, while the guanidine group of Arg 59 makes double hydrogen bonds to Asp 368. In an effort to further our understanding of the structural features lending to the bioactivity of batzelladines and analogues, we carried out modeling studies of inhibitors binding to gp120. Mindful of the structural features of CD4-gp120 binding and the structure−activity relationships gleaned from the HIV-1 fusion assays, modeling was accomplished by docking and minimization of the complexes between gp120 and several of the batzelladine analogues as described next.

We began the modeling studies with compound **27**, which is representative of the bistricyclic guanidines found to be the best inhibitors. The structure of **27** was first minimized and then positioned randomly about 20 Å outside of the CD4bs (Figure 5a). Manual docking attempts demonstrated to us that the shape and concavity of the CD4bs would require that the inhibitor occupy a nearly horizontal position in the view seen in Figure 5a,c. That is, the overlying residues of the CD4bs preclude docking the bisguanidines in a more-nearly vertical orientation. Thus, as seen in Figure 5b, four possible modes of binding could occur owing to the presence of two guanidine ring systems and two possible binding orientations. In generating a set of distance restraints that would facilitate electrostatic interactions, we made the assumption that either of the guanidine units residing within the two tricyclic motifs in **27** would mimic the guanidine group of the side chain of Arg69 and participate in electrostatic interactions with Asp368 of gp120. Thus, four sets of distance restraints that account for the four possible orientations of the ligand were prepared. To allow the program to sample all four binding orientations (Figure 5b), these restraints were initially introduced as ambiguous distance restraints, where restraints are satisfied as long as one of the four sets of distances is satisfied. For compound **27**, the structures converged surprisingly well (∼80%) to orientation 3 (lower left panel), where the guanidine group of the terminal ring system is within hydrogen-bonding distance of the carboxylate of Asp368. Of the remaining 20% of the structures, the majority converged to orientation 4. Owing to the proximity to gp120 of the alkyl groups positioned on ring B or D in orientations 1 and 2, respectively, it was impossible to position the guanidine units near Asp368 of gp120 without other portions of the ligand making bad contacts with gp120, even among the multiple conformations observed for the alkyl chains. Additional calculations were then carried out for **27** bound to gp120 in orientation 3 wherein conservative and ambiguous restraints were introduced so as to allow favorable van der Waals interactions between any hydrophobic region of compound **27** and gp120. The family of structures for which no violations were observed was subsequently averaged, and the restrained regularized mean structure of **27** docked to gp120 is shown in Figure 5c. From the model, it appears likely that this conformation can facilitate hydrophobic interactions between the ligand and the V1/V2 stem loop of gp120, which comprises predominantly hydrophobic amino acids.

These results led us to next examine the effect of stereochemistry of the terminal guanidine ring system on the model since several different arrangements are present in compounds **25**−**30**, all of which are good inhibitors. Compound **28**, which has the opposite configuration of the left-hand guanidine unit of that of **27**, was therefore minimized, docked, and subjected to torsion angle dynamics using the same protocol as that used for the model of **27**. Results similar to those obtained for compound **27** were observed for **28**, where the structures largely converged to orientation 3. Although the opposite stereochemistry leads to a pucker of the tricyclic ring system opposite that of **28**, the pyrrole is directed to the outside of the CD4 binding site, and modeling suggests that the large binding pocket (relative to the tricyclic guanidine motif) can accommodate either shape.

Table 2. Energies[a] of Compound **27** upon Binding to gp120

orientation	VDW	torsion	dipole−dipole	total
3	11.3	14.6	2.3	28.2
4	14.3	28.6	3.0	45.9

[a] kcal mol^{-1}.

Before moving on to other analogues, we sought to further examine the alternate binding mode (orientation 4, Figure 5b) where the central (comprising rings C/D), rather than the terminal (rings A/B), guanidine motif is centered in the CD4bs. We therefore carried out additional calculations again including ambiguous distance restraints that would allow for favorable protein−ligand interactions. Although a model for **27** binding to gp120 in this alternate mode could be obtained (model presented in Supporting Information), the torsion angle and van der Waals energies of the ligand bound in this mode were approximately double those obtained for **27** binding in orientation 3 (Table 2).

Following on the results of docking and modeling for compounds **27** and **28**, we also attempted to dock compounds **33** and **37**, which showed little to no activity. After numerous attempts, however, we were unable to model either of these compounds into the CD4bs on gp120, even if we positioned the analogues (in each of the four possible orientations) near the CD4bs by hand. As discussed above, compounds **31**−**38** differ from **25**−**30** in that the methyl group at C-1 has been replaced by an additional C_7 or C_9 alkyl chain. With respect to accessibility to the guanidine nitrogens, the net result is that each guanidine motif bears two or more bulky substituents at C-1/C-1′ and/or C-2/C-2′, obstructing these compounds from entering deeply enough into the binding pocket to participate in hydrogen-bonding interactions with Asp368. Compounds **37** and **38**, both of which possess a methyl phenyl bis ester linkage, were the worst inhibitors of this library and failed to inhibit fusion even at 1 mM concentrations (data not shown). This implies that the imposed rigidity of the methyl phenyl linker, the added mass between the guanidine motifs, or both abrogate fusion-blocking activity. We were also unsuccessful with docking either of these compounds to the CD4bs.

Conclusions

The crystal structures of gp120 solved to date are all ternary complexes between the gp120 core, CD4, and anti-gp120 antibody.[18,19] The construct used for crystallization of gp120 comprises what are believed to be the three domains corresponding to the central core of gp120 and the stem of the V1/V2 loop. In terms of binding affinity, interactions between this core gp120 molecule and both CD4 and anti-gp120 antibodies are preserved, evidence that this construct truly represents the main structural features of gp120. In this study we have carried out HIV-1 fusion assays and modeled batzelladine analogues binding to the CD4bs of gp120 by docking and minimization. Clear structure−activity relationships were revealed from the

fusion assay data and indicated that inhibitors with low to sub-micromolar IC_{50} values incorporate two tricyclic guanidine ring systems tethered by a flexible alkyl linker wherein C-1 of the terminal guanidine motif is substituted by a methyl group only. Consistent with these results, modeling studies of compounds representing the best and worst fusion inhibitors demonstrated that a terminal tricyclic guanidine motif, lacking substitution at C-1, converged to one preferred orientation of binding to the CD4bs on gp120, permitting electrostatic interactions between the guanidine nitrogens and the carboxylate of Asp368, as well as extensive hydrophobic interactions between the alkyl chains and predominantly hydrophobic regions of gp120. Compounds comprising essentially one-half of the bisguanidines were less potent inhibitors of fusion than the so-called dimers. These monomers can be docked to the CD4bs in a similar manner as compounds **25**−**30**, but lack the second alkyl unit that likely contributes favorable hydrophobic interactions. These studies therefore provide another example whereby dimerization of ligands enhances potency[20,21] and provide a structural framework for further development of useful HIV-1 fusion inhibitors.

Experimental Section

HIV-1 Env-Mediated Fusion Assays. Assays were carried out in duplicate on at least two separate days for both LAV and SF162 viruses using protocols identical to those already described.[22] In the single-concentration assays, inhibitors were added to each well to a final concentration of either 100 or 5 μM. For dose−response experiments, inhibitors were added in increasing concentrations to each well and inhibition curves were best fit to the equation % fusion = $100/(1 + K_A[I])$ where [I] is the concentration of inhibitor and K_A is the equilibrium association constant for inhibitor binding to gp120. Curves were fit by nonlinear least-squares optimization using the program Kaleidagraph 3.5 (Synergy Software, Reading, PA).

Modeling of Inhibitor-gp120 Complexes. Three-dimensional coordinates for inhibitors used in this study were generated using the program Chem3D. Parameter and topology files for each set of coordinates were subsequently autogenerated using the program XPLO2D[23] and minimized using the program Xplor-NIH.[24] Inhibitors were randomly positioned approximately 20 Å from the CD4bs on gp120 using the program GRASP,[25] and models were obtained by conjoined rigid body/torsion angle dynamics.[26,27] During the dynamics protocol, gp120 is treated as a fixed rigid body (that is, the coordinates for gp120 are held fixed), while the inhibitor is free to translate and rotate relative to the protein, and the alkyl chain and linker are given torsional degrees of freedom. Force constants for bonds, angles, and impropers were set to 1000, 500, and 750 kcal mol^{-1}, respectively. Note that no dihedral angle force constants were employed since dihedral angles are either held fixed or allowed free rotation if residing within the alkyl chains or linker. Force constants for distance restraints were increased from 2 to 30 kcal mol^{-1} during the course of the run. Each restrained minimized model was derived from the average of a set of 20 structures for which no intermolecular distance violations greater than 0.3 Å or dihedral angle violations (corresponding to those angles that were fixed) greater than 5° were observed.

Acknowledgment. This work was supported in part by the Intramural AIDS Targeted Antiviral Program of the Office of the Director, National Institutes of Health (C.A.B.) and NIH grant HL-25854 (L.E.O.).

Supporting Information Available: The source of the batzelladine analogues studied and experimental procedures for preparing **17**−**19**, **21**, and **27** together with characterization data for these compounds; figure illustrating model of **27** in complex with gp120 in orientation 4. This material is available free of charge via the Internet at http://pubs.acs.org.

References and Notes

(1) Kashman, Y.; Hirsh, S.; McConnell, O. J.; Ohtani, I.; Kusumi, T.; Kakisawa, H. *J. Am. Chem. Soc.* **1989**, *111*, 8925−8926.
(2) Jares-Erijman, E. A.; Sakai, R.; Rinehart, K. L. *J. Org. Chem.* **1991**, *56*, 5712−5715.
(3) Jares-Erijman, E. A.; Ingrum, A. L.; Carney, J. R.; Rinehart, K. L.; Sakai, R. J. *J. Org. Chem.* **1993**, *58*, 4805−4808.
(4) Berlinck, R. G. S.; Braekman, J. C.; Daloze, D.; Bruno, I.; Riccio, R.; Ferri, S.; Spampinato, S.; Speroni, E. *J. Nat. Prod.* **1993**, *56*, 1007−1015.
(5) Chang, L.-C.; Whittaker, N. F.; Bewley, C. A. *J. Nat. Prod.* **2003**, *66*, 1490−1494.
(6) Patil, A. D.; Kumar, N. V.; Kokke, W. C.; Bean, M. F.; Freyer, A. J.; De Brosse, C.; Mai, S.; Truneh, A.; Faulkner, D. J.; Carte, B.; Breen, A. L.; Hertzberg, R. P.; Johnson, R. K.; Westley, J. W.; Potts, B. C. M. *J. Org. Chem.* **1995**, *60*, 1182−1188.
(7) Patil, A. D.; Freyer, A. J.; Taylor, P. B.; Carté, B.; Zuber, G.; Johnson, R. K.; Faulkner, D. J. *J. Org. Chem.* **1997**, *62*, 1814−1819.
(8) Palagiano, E.; Demarino, S.; Minale, L.; Riccio, R.; Zollo, F.; Iorizzi, M.; Carre, J. B.; Debitus, C.; Lucarain, L.; Provost, J. *Tetrahedron* **1995**, *51*, 3675−3682.
(9) Snider, B. B.; Chen, J. S.; Patil, A. D.; Freyer, A. J. *Tetrahedron Lett.* **1996**, *37*, 6977−6980.
(10) Black, G. P.; Murphy, P. J.; Walshe, N. D. A. *Tetrahedron* **1998**, *54*, 9481−9488.
(11) Overman, L. E.; Rabinowitz, M. H.; Renhowe, P. A. *J. Am. Chem. Soc.* **1995**, *117*, 2657−2658.
(12) Nagasawa, K.; Georgieva, A.; Koshino, H.; Nakata, T.; Kita, T.; Hashimoto, Y. *Org. Lett.* **2002**, *4*, 177−180.
(13) Reviewed in: Aron, Z. D.; Overman, L. E. *Chem. Commun.* **2004**, in press.
(14) Cohen, F.; Collins, S. K.; Overman, L. E. *Org. Lett.* **2003**, *5*, 4485−4488.
(15) Cohen, F.; Overman, L. E. *J. Am. Chem. Soc.* **2001**, *123*, 10782−10783.
(16) Nussbaum, O.; Broder, C. C.; Berger, E. A. *J. Virol.* **1994**, *68*, 5411−5422. Salzwedel, K.; Smith, E. D.; Dey, B.; Berger, E. A. *J. Virol.* **2000**, *74*, 326−333.
(17) Reviewed in: Berger, E. A.; Murphy, P. M.; Farber, J. M. *Annu. Rev. Immunol.* **1999**, *17*, 657−700.
(18) Kwong, P. D.; Wyatt, R.; Robinson, J.; Sweet, R. W.; Sodroski, J.; Hendrickson, W. A. *Nature* **1998**, *393*, 648−659.
(19) Kwong, P. D.; Wyatt, R.; Majeed, S.; Robinson, J.; Sweet, R. W.; Sodroski, J.; Hendrickson, W. A. *Struct. Fold. Des.* **2000**, *8*, 1329−1339.
(20) Carlier, P. R.; Du, D. M.; Han, Y. F.; Liu, J.; Perola, E.; Williams, I. D.; Pang, Y. P. *Angew. Chem., Int. Ed.* **2000**, *39*, 1775−1777.
(21) Carlier, P. R.; Cho, E. S.; Han, Y.; Liu, J.; El Yazal, J.; Pang, Y. P. *J. Med. Chem.* **1999**, *42*, 4225−4231.
(22) Louis, J. L.; Nesheiwat, I.; Chang, L. C.; Clore, G. M.; Bewley, C. A. *J. Biol. Chem.* **2003**, *278*, 20278−20285.
(23) Kleywegt, G. T.; Jones, T. A. *Methods Enzymol.* **1997**, *277*, 208−230.
(24) Schwieters, C. D.; Kuszewski, J. J.; Tjandra, N.; Clore, G. M. *J. Magn. Reson.* **2003**, *160*, 66−74.
(25) Nichols, A.; Sharp, K. A.; Honig, B. *Proteins Struct. Func. Genet.* **1991**, *11*, 281−296.
(26) Bewley, C. A.; Clore, G. M. *J. Am. Chem. Soc.* **2000**, *122*, 6009−6016.
(27) Schwieters, C. D.; Clore, G. M. *J. Magn. Reson.* **2001**, *152*, 288−302.

NP049958O